Science of the Total Environment 871 (2023) 162050

Contents lists available at ScienceDirect

Science of the Total Environment

journal homepage: www.elsevier.com/locate/scitotenv

Foam fractionation for removal of per- and polyfluoroalkyl substances: Towards closing the mass balance

Sanne J. Smith [a,*], Jeffrey Lewis [b], Karin Wiberg [a], Erik Wall [c], Lutz Ahrens [a]

[a] Department of Aquatic Sciences and Assessment, Swedish University of Agricultural Sciences (SLU), P.O. Box 7050, SE-750 07 Uppsala, Sweden
[b] ECT2, Lärlingsgatan 14b, SE-90422 Umeå, Sweden
[c] Cytiva, Björkgatan 30, SE-75323 Uppsala, Sweden

HIGHLIGHTS

- Foam fractionation could remove PFAS from industrial water on pilot-scale.
- Air emissions were high, but no major contributor to low mass-balance closures.
- Airborne PFAS caused an occupational exposure that exceeds the EFSA recommendation.
- Removal correlated positively with total element concentration and conductivity.

GRAPHICAL ABSTRACT

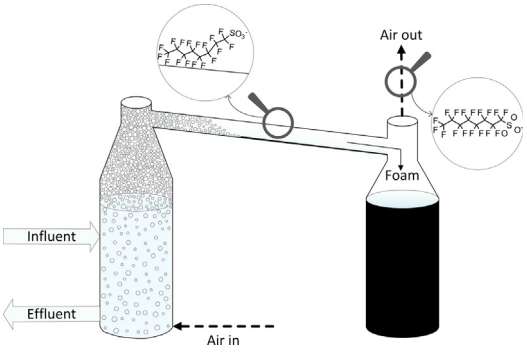

ARTICLE INFO

Guest Editor: Vitor Vilar

Keywords:
Per- and polyfluoroalkyl substances (PFAS)
Water treatment
Air emissions
Foam fractionation
Pilot-scale
Remediation

ABSTRACT

Foam fractionation has recently attracted attention as a low-cost and environmentally benign treatment technology for water contaminated with per- and polyfluoroalkyl substances (PFAS). However, data on the mass balance over the foam fractionation process are scarce and when available, gaps in the mass balance are often identified. This study verified the high treatment efficiency of a pilot-scale foam fractionation system for removal of PFAS from industrial water contaminated with aqueous film-forming foam. ΣPFAS removal reached up to 84 % and the removal of perfluorooctane sulfonic acid (PFOS) up to 97 %, but the short-chain perfluorobutanoic acid (PFBA) was only removed with a mean efficiency of 1.5 %. In general, mobile short-chain PFAS were removed less efficiently when the perfluorocarbon chain length was below six for carboxylic acids and below five for sulfonic acids. Fluctuations in treatment efficiency due to natural variations in the chemistry of the influent water were minor, confirming the robustness of the technology, but significant positive correlations between PFAS removal and influent metal concentration and conductivity were observed. Over all experiments, the mass balance closure did not differ significantly from 100 %. Nonetheless, PFAS sorption to the walls of the reactor was measured, as well as high PFAS emissions by the air exiting the reactor. PFAS emissions in aerosols correlated positively with mass balance closure. The elevated aerial PFAS concentrations measured in the experimental facility have implications for worker safety and prevention of PFAS-emissions to the atmosphere, and demonstrate the importance of installing appropriate filters on the air outlet of foam fractionation systems.

1. Introduction

Per- and polyfluoroalkyl substances (PFAS) are exceptionally stable anthropogenic chemicals with versatile applications as lubricants, coatings and surfactants (Buck et al., 2011; Evich et al., 2022). The widespread

* Corresponding author.
E-mail address: sanne.smith@slu.se (S.J. Smith).

http://dx.doi.org/10.1016/j.scitotenv.2023.162050
Received 18 August 2022; Received in revised form 1 February 2023; Accepted 2 February 2023
Available online 7 February 2023

use, high mobility and persistent nature of PFAS has caused their ubiquitous presence in the environment, ultimately leading to human exposure to these chemicals via contaminated air, water or food (Sunderland et al., 2019). The toxicology of most PFAS is still poorly understood, although numerous health impacts have been demonstrated for legacy compounds such as perfluoroalkyl carboxylic acids (PFCA) and perfluorosulfonic acids (PFSA) (Fenton et al., 2020). Because of these findings, health-based guidelines for PFAS exposure have been introduced in e.g. the U.S. and Europe (EFSA, 2020; US EPA, 2016).

To adequately limit human exposure to PFAS, the development of cost-efficient remediation technologies for contaminated sources is urgently needed. The use of PFAS-containing aqueous film-forming foams (AFFF) constitutes an important source of these chemicals, causing contamination of soil, groundwater and surface water (Ahrens, 2011; Lenka et al., 2021; Sunderland et al., 2019). Treating AFFF-contaminated water before discharge is hence crucial towards preventing the spread of PFAS in the environment. Numerous treatment methods exist that are being applied on full-scale, of which adsorption to granular activated carbon (GAC) (Belkouteb et al., 2020), ion exchange resins (IEX) (Dixit et al., 2021) or foam fractionation (Burns et al., 2021) are used most often.

Of these three treatment technologies, foam fractionation has the advantage that no consumables are used during the process, generating very low operating expenses (Burns et al., 2021). Moreover, since no regeneration of sorbent materials using thermal treatment or organic solvents is necessary, the treatment can be considered environmentally benign. The process has been well-described in academic literature for the removal of PFAS (Buckley et al., 2022, 2021; Burns et al., 2021; Lee et al., 2017; McCleaf et al., 2021; Meng et al., 2018; Smith et al., 2022). In essence, it is similar to conventional sorption processes, but the sorbent consists of rising air bubbles that are introduced at the bottom of a water column. Because most PFAS are amphiphilic, they adsorb to the surface of these air bubbles, with their polar parts remaining in the water phase and their apolar tails inside the air bubble. If enough surfactant molecules are present, a PFAS-enriched foam will form on top of the water, which can be harvested as foamate and treated further separately. Conversely, the bulk water phase will be depleted of PFAS.

The effectiveness of foam fractionation towards the removal of long-chain PFAS (i.e. PFSA: $C_nF_{2n+1}SO_3H$, $n > 5$; PFCA: $C_nF_{2n+1}COOH$, $n > 6$) has been documented extensively, with removal efficiencies generally exceeding 95 % (Buckley et al., 2022; Burns et al., 2021; Lee et al., 2017; McCleaf et al., 2021; Meng et al., 2018). However, foam fractionation is less suitable for the removal of the more mobile short-chain PFAS, because these compounds have lower air-water sorption coefficients (Buckley et al., 2022; Burns et al., 2021). Moreover, various studies report a loss of PFAS in the overall mass balance, with up to 36 % less PFAS measured in the foamate than was removed from the water phase (McCleaf et al., 2021; Smith et al., 2022). It is unclear whether these missing PFAS are emitted to the air, adsorb to the reactor walls or are transformed during the treatment process. Finally, effects of natural variations in the chemistry of the influent water are still poorly understood.

To assess these knowledge gaps, the current study aimed to investigate the mass balance of the foam fractionation process, as well as verify the performance of the treatment. Specifically, objectives were to *i)* explore the effect of residence time, surfactant dosage, conductivity and metal and total organic carbon (TOC) concentration on the PFAS removal using a pilot-scale continuous foam fractionation reactor treating an industrial AFFF-contaminated water stream with highly variable composition, *ii)* comprehensively examine the PFAS mass balance over the influent, effluent and foam and *iii)* evaluate whether PFAS are present in the air and aerosols that exit this pilot-scale foam fractionation reactor and if this could explain any gaps in the mass balance.

2. Methods

The brands and purity grades of all chemicals can be found in Table SI 1. All glassware was burned at 400 °C overnight and all glass or plastic containers were rinsed three times with the appropriate solvent before use. Full names of all PFAS compounds are given in Tables SI 2 and SI 3.

2.1. Experimental approach

A pilot-scale continuous foam fractionation system designed by ECT2 (Emerging Compounds Treatment Technologies, Sweden) was used in all experiments to treat PFAS-contaminated industrial water at Cytiva, Uppsala, Sweden. This water consisted of a mixture of AFFF-contaminated surface runoff, groundwater and process water with a variable composition, collected continuously in a 12 m^3 storage filled to 50 % capacity prior to entering the on-site water treatment system. The water was pumped directly from this tank into the foam fractionating system, so PFAS concentrations and other chemical parameters in the influent varied over time. A schematic overview of the process is given in Fig. 1. Water continuously entered the foam fractionation column (Ø 49.4 cm, water level at 108.5 cm) at a height of 92 cm above the column bottom and exited the column at the bottom. A venturi blower was used for introducing air bubbles to the water in a recirculation loop. To enhance foaming, a constant flow of soap (Neutral® Hand Dishwash, Unilever, ingredients: 5–15 % anionic surfactants, <5 % amphoteric surfactants, non-ionic surfactants, sodium benzoate) solution in influent water was supplied to the venturi system using a peristaltic pump (Masterflex L/S with neoprene tubing). Once the foam rose to the top of the system at approximately 60 cm above the water level, it was forced to collapse under warm air that entered the system through a heater. The liquid foamate then flowed down a pipe into a foam collection vessel. A fan blowing air out of the system was placed on top of the foam vessel, to improve the foam flow.

Duplicate foam fractionation runs at various residence times (13, 20, 30 and 60 min) and soap ratios (21, 62 and 125 ppmv) were carried out to assess the PFAS removal efficiency of the system, see Table 1 for details. The soap ratio is the ratio between the pure soap dosage rate to the venturi and the influent water flow rate. For each experiment, the system was run for 1 h after the foam flow started, except for the experiments at 60 min residence time, which were run for 2 h. The foam flow rate was observed to remain relatively constant over the duration of each experiment. 250 mL influent was collected before and after each run in clean polypropylene (PP) bottles from a valve in the influent hose for determination of PFAS concentrations, pH and conductivity, to correct for the variability of the influent during the experiment. 250 mL effluent and foam were collected for PFAS analysis at the end of each run. Moreover, 500 mL influent was collected at the end of each experiment for determination of the TOC and metal concentrations.

All experimental duplicates were carried out directly after each other, to minimize variations in the influent. Two of the experiments were repeated in duplicate one week later, to assess the effect of differences in influent water characteristics. Before each experiment, the column was flushed with at least three column volumes of influent water in the absence of air flow to clean the system. After each experiment, all foam was pumped out of the foam collection vessel with a peristaltic pump (Watson Marlow, 630SN/RE with Pureweld Xl 12.7 mm tubing) and weighed to determine the amount of foam produced. Foam samples were taken from this bulk foam. At the end of the experimental period, the pipe through which the foam flowed to the collection vessel was rinsed with MilliQ water and ethanol, which was combined and sent in for PFAS analysis to check for PFAS sorption to the pipe walls.

2.2. Air and aerosol sampling

An aluminum air sampler holder (Tisch Environmental, pre-cleaned with acetone) containing two pre-combusted stacked quartz microfiber filters (⌀ 11 cm, pore size 2.2 μm, QM-A, Whatman) was placed above the fan (see Fig. 1), to collect aerosols in the air exiting the system. To ensure detectable PFAS concentrations, the filters were only replaced after each set of duplicates rather than between duplicates as well. There was a space of approximately 5 mm between the sampler and the air exit, so not all air

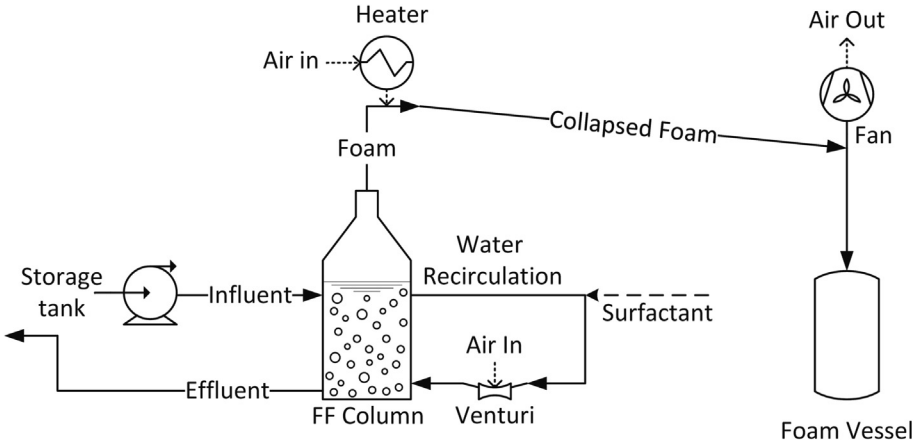

Fig. 1. Process overview of the single-stage pilot-scale continuous foam fractionation reactor employed in this study. The conical-shaped top part of the column filled up with foam, which subsequently flowed down into the foam collection vessel.

passed through the filters, because otherwise the air flow through the fan was inhibited too much. The minimum air flow was found by detecting the point where foam collection system did not work properly anymore, causing low foam flows and incomplete collapse of the foam. In the repeated run of experiment 1, the aerosol sampler was placed upside down, such that the distance between the air outlet and the filter was decreased from approximately 9 cm to 4 cm.

To sample the PFAS content in the air around the foam fractionation reactor, four passive air samplers (PAS; Tisch Environmental) containing sorbent-impregnated polyurethane foam discs (SIPs) were employed in the same room as the reactor during all experiments, over a total duration of eleven days. The approximate placement of these four PAS-SIPs is shown in Fig. SI 1. The use of SIPs for PFAS detection in air is a well-established method that has been developed and verified extensively in earlier studies (Ahrens et al., 2013; Shoeib et al., 2008; Winkens et al., 2017). An additional PAS-SIP was employed in the staircase of the same building as a reference location for the background indoor environment. A field blank was collected by placing a SIP inside the PAS housing for one minute on-site, after which the SIP was treated as all other samples. All PAS housings had been cleaned with tap water followed by thorough rinsing with acetone prior to employment and SIPs were only handled using acetone-rinsed tweezers.

The SIPs were prepared according to the protocol by Ahrens et al. (2013). In brief, polyurethane foam discs (PUFs, Tisch Environmental, 0.5 × 5.5″) were cleaned by Soxhlet extraction with acetone for 24 h, followed by petroleum ether for 17 h and fresh petroleum ether for 7 h. Finely ground XAD-4 resin was Soxhlet extracted with methanol for 17 h, followed by dichloromethane for 24 h and hexane for 6 h. The clean XAD-4 was kept in a beaker at −20 °C, while the PUFs were dried in a pre-cleaned vacuum desiccator for approximately 72 h. After drying, the PUFs were impregnated by dipping them in a XAD-4 in hexane slurry (approximately 6.4 g L^{-1}) three times for 30 s and subsequent drying on a heating plate, both repeated twice. After the second drying step, the SIPs were dried further in a vacuum desiccator again for 72 h. Prior to transport, the SIPs were wrapped in pre-cleaned aluminum foil and stored in individual airtight zip-lock bags.

2.3. Chemical analyses

All water samples were shipped to ALS Scandinavia for PFAS ($n = 32$, *Table SI 2*), TOC, turbidity and metal and element content analysis. For the PFAS analysis, a laboratory blank of 250 mL MilliQ water, a field blank of 250 mL MilliQ water, which was opened on-site for 1 min, and a surfactant blank of approximately 5 g/L surfactant in MilliQ water were sent in as well. Limits of quantification (LOQ) of individual PFAS in the analytical method varied between 0.01 and 25 μg L^{-1}, depending on the PFAS compound and the matrix, and are given in Table SI 2. An overview of the metals and elements included in the analysis with their quantification limits is given in Table SI 4. pH and conductivity of the influent were measured on-site using a Knick Memosens 555 pH sensor and Hach CDC401 conductivity probe, respectively.

The quartz microfiber filters used for aerosol collection and the PAS-SIPs were analyzed in the laboratory at the Department of Aquatic Sciences and Assessment, Swedish University of Agricultural Sciences. The extraction was carried out according to a modified protocol described by Casas et al. (2020). One blank without filter and one blank with a clean filter were included in addition to the field blank. Each filter was transferred to a 50 mL PP vial and spiked with 50 μL of an internal standard (IS) mixture containing 50 ng mL^{-1} of each individual compound (Smith et al., 2022). 15 mL of methanol was added, after which the tubes were vortexed and sonicated for 20 min. The methanol was decanted into a second tube, and the extraction was repeated twice with 5 mL of methanol. The combined methanol fractions were concentrated to 0.5 mL under a gentle stream of N_2 and transferred to 1.5 mL Eppendorf tubes. The PP tubes were rinsed

Table 1
Overview of experimental parameters. Experiments 1 and 2 (E1 and E2) were repeated twice (R1 and R2), one week apart, to assess the effect of a different influent water quality. In E1 R2, the distance between the air outlet and the aerosol filters was decreased. The soap ratio is the ratio between the volumetric dish-soap dosage rate and the influent water flow rate. Since the surfactant concentration of the dish-soap was 5–15 %, the pure soap ratio was between 1.05 and 3.15 ppmv for a soap ratio of 21 ppmv, between 3.1 and 9.3 ppmv for a soap ratio of 62 and between 6.25 and 18.8 for a soap ratio of 125.

Experiment ID	Contact time (min)	Water flow rate (L/min)	Soap dilution factor	Soap solution flow rate (mL/min)	Soap ratio (ppmv)	Run time (h)
E1 R1, E1 R2	30	6.9	250	36	21	1
E2 R1, E2 R2	20	10	250	54	21	1
E3	13	16	250	83	21	1
E4	60	3.5	83	18	62	2
E5	20	10	83	54	62	1
E6	20	10	42	54	125	1

three times with methanol, which was added to the same Eppendorf tubes, and the extracts were concentrated to 0.5 mL again. Then, the tubes were centrifuged for 15 min at 4000 rpm (Eppendorf centrifuge 5424R) and 150 μL supernatant was transferred to an analytical PP insert vial.

Prior to the extraction of the SIPs (Ahrens et al., 2013), extraction thimbles (Munktell Ahlstrom, ET/MG 160, 33 × 80 mm) were cleaned by Soxhlet extraction with 350 mL methanol for 18 h, followed by 350 mL of a 1:1 acetone:diethyl ether mixture for 24 h. Then, each SIP was added into a cleaned extraction thimble and Soxhlet extracted with 330 mL methanol for 24 h. A solvent blank without thimble and SIP was included in addition to the field blank. Each extract was concentrated to approximately 4 mL using rotary evaporation and transferred to a pre-cleaned 15 mL PP tube. The round-bottomed flask used during the Soxhlet extraction followed by rotary evaporation was rinsed three times with methanol, which was added to the extract, and the extracts were concentrated to 0.5 mL under N_2. Subsequently, the tubes were centrifuged for 20 min at 3900 rpm (Eppendorf centrifuge 5810R) and 150 μL supernatant was transferred to an analytical PP insert vial. Finally, the filter and SIP extracts were analyzed for 29 PFAS on a Sciex 3500 UPLC-MS/MS system according a modified method described previously (Smith et al., 2022) and in the SI (page 3).

2.4. Data handling

Concentrations of individual PFAS and elements that were not detected in any of the samples were set to zero. Other non-detect compounds, i.e. PFAS or elements that were present above the LOQ in at least one sample, were given a concentration equal to half their LOQ. For the water samples, LOQs of individual PFAS varied depending on the water matrix and were occasionally higher in the influent as compared to the effluent samples. In this case, the removal would increase by as much as 10 % points if non-detect concentrations were set equal to their LOQ. On the other end, setting all non-detect PFAS concentrations to zero was also deemed unrealistic, hence a factor 0.5 was chosen. Nonetheless, it should be acknowledged that this choice affects the results, and a sensitivity analysis in the form of repeated plots for factors 0 and 1 is given in the SI. Furthermore, most important statistical relationships are based on ΣPFAS concentrations as well as PFOS concentrations, since PFOS was the only PFAS present above the LOQ in all samples and thus unaffected by this choice. LOQs in the air and aerosol samples were set to the maximum concentration recovered in any of the field or lab blanks and are given in Table SI 3. For compounds that were not detected in any blanks, the instrument LOQ of 0.1 ng per filter or SIP was used. SIP and aerosol filter concentrations were not blank-corrected and values below the LOQ were set to half the LOQ. Air concentrations were estimated by assuming a common linear air sampling rate of 4 $m^3\ d^{-1}$, as described in Ahrens et al. (2013), resulting in a total air volume sampled of 44 m^3 per SIP.

Mean removal efficiencies (RE) for each experiment were calculated as per Eq. (1), with C_{Ef} the mean effluent PFAS water concentration over both duplicates (n = 2) and C_{In} the mean of the influent water concentrations measured before and after the experiment for both duplicates (n = 4). Similarly, mean mass balance closures (MB) were calculated as per Eq. (2), with C_{Foam} the mean foam PFAS concentration over both duplicates (n = 2) and $\%_{Foam}$ the mean foam fraction (%). The foam fraction was calculated by dividing the total mass of collapsed foam collected at the end of each experiment by the total volume of water treated. It should be acknowledged that this calculation is an approximation, because the foam concentration was based on a time-integrated sample over the entire experiment, whereas the effluent concentration was only measured at the end during steady-state operation. Moreover, the measurement uncertainties in the influent flow rate as well as the foam volume deserve consideration. An unsteady state analysis over the foam concentration is provided in SI Section 2 (p. 5–7), which showed that although the mean theoretical error caused by sampling the bulk foam was 30 %, the magnitude of this error did not correlate significantly with the mass balance. Hence, the combined effect of analytical uncertainty in PFAS concentrations, uncertainty in the measured flows and degradation of precursors contributed more to the mass balance uncertainty than this theoretical error. All data analysis and plotting were done in Matlab™, version R2020b.

$$RE\ (\%) = 100 - \frac{C_{Ef}}{C_{In}} \cdot 100 \tag{1}$$

$$MB\ (\%) = \frac{\frac{\%_{Foam}}{100} \cdot C_{Foam} + \left(1 - \frac{\%_{Foam}}{100}\right) \cdot C_{Ef}}{C_{In}} \cdot 100 \tag{2}$$

3. Results and discussion

3.1. Characteristics of influent water

The mean influent ΣPFAS concentration with corresponding standard deviation was 15 ± 3.9 μg L^{-1}, with PFOS (7.6 ± 2.6 μg L^{-1}), PFHxS (1.7 ± 0.51 μg L^{-1}) and 6:2 FTSA (1.3 ± 0.41 μg L^{-1}) as major components. A complete overview of the mean influent concentrations of all detected compounds is given in Table SI 5. Mean TOC, turbidity, pH, conductivity, aluminum and iron concentrations were 8.5 ± 0.6 mg L^{-1}, 21 ± 24 FNU, 7.4 ± 0.1, 1300 ± 190 μS cm^{-1}, 150 ± 97 μg L^{-1} and 790 ± 560 μg L^{-1}, with a complete overview given in Table SI 5. These values show the high variation in the quality of the industrial water stream under investigation, with relative errors exceeding 100 % for certain parameters.

Based on the mean influent concentrations of all eight experiments, significant positive correlations between influent ΣPFAS as well as PFOS concentration and aluminum (Al), boron (B), barium (Ba), calcium (Ca), iron (Fe), potassium (K), lithium (Li), magnesium (Mg), silicon (Si) and strontium (Sr) were found, with Pearson r values ranging from 0.74 (Sr) to 0.85 (Ba) for PFOS and from 0.73 (Al) to 0.93 (Si and Ba) for ΣPFAS. Conversely, both influent ΣPFAS and PFOS concentrations significantly correlated negatively ($p < 0.05$, $r = -0.90$ and -0.78, respectively) with P concentration. P and Zn correlated positively with each other, but negatively with B, Ca, Li, Mg, Si and Sr. An overview of all correlation coefficients is given in Fig. SI 4. These trends indicate that at least two distinct sources contributed to the process water, one with higher P and Zn, lower PFAS and lower other metal concentrations compared to the other, and the overall composition of the influent water depends on the ratio of these two contributing flows.

3.2. PFAS removal in different experiments

Between experiments, the ΣPFAS removal efficiency (RE) ranged from 63 to 84 %, as illustrated in Fig. 2. Increasing the relative surfactant dosage lead to higher foam fractions, with mean foam fractions of 0.17 %, 1.1 % and 7.1 % at soap ratios of 21, 62 and 125 ppmv, respectively (only significant between ratios of 62 and 125 ppmv, 1-way ANOVA, $F(2,5) = 82.53$, $p = 0.0001$). However, higher foam fractions did not correlate significantly with higher ΣPFAS or PFOS removal and ΣPFAS removal efficiencies above 80 % were already achieved at foam fractions below 0.5 %, see Fig. 2A), B) and F). This result is extremely relevant for practical applications of the foam fractionation technology, because it means that competitive PFAS removal can be achieved with up to 1400-fold reductions in water volume. Certain commercial applications of foam fractionation for PFAS remediation use a multistage treatment (Burns et al., 2021), where the foam undergoes subsequent foam fractionation to achieve higher concentration factors. Depending on the costs for foam treatment, including additional foam fractionation stages could be worthwhile for the current system as well.

The RE was significantly higher at 20, 30 and 60 min contact time (t_c) as compared to 13 min, but no significant differences in RE between 20, 30 and 60 min t_c were found (one-way ANOVA, $F(3,4) = 25.55$, $p = 0.005$ followed by Tukey's hsd procedure). This result is in accordance with

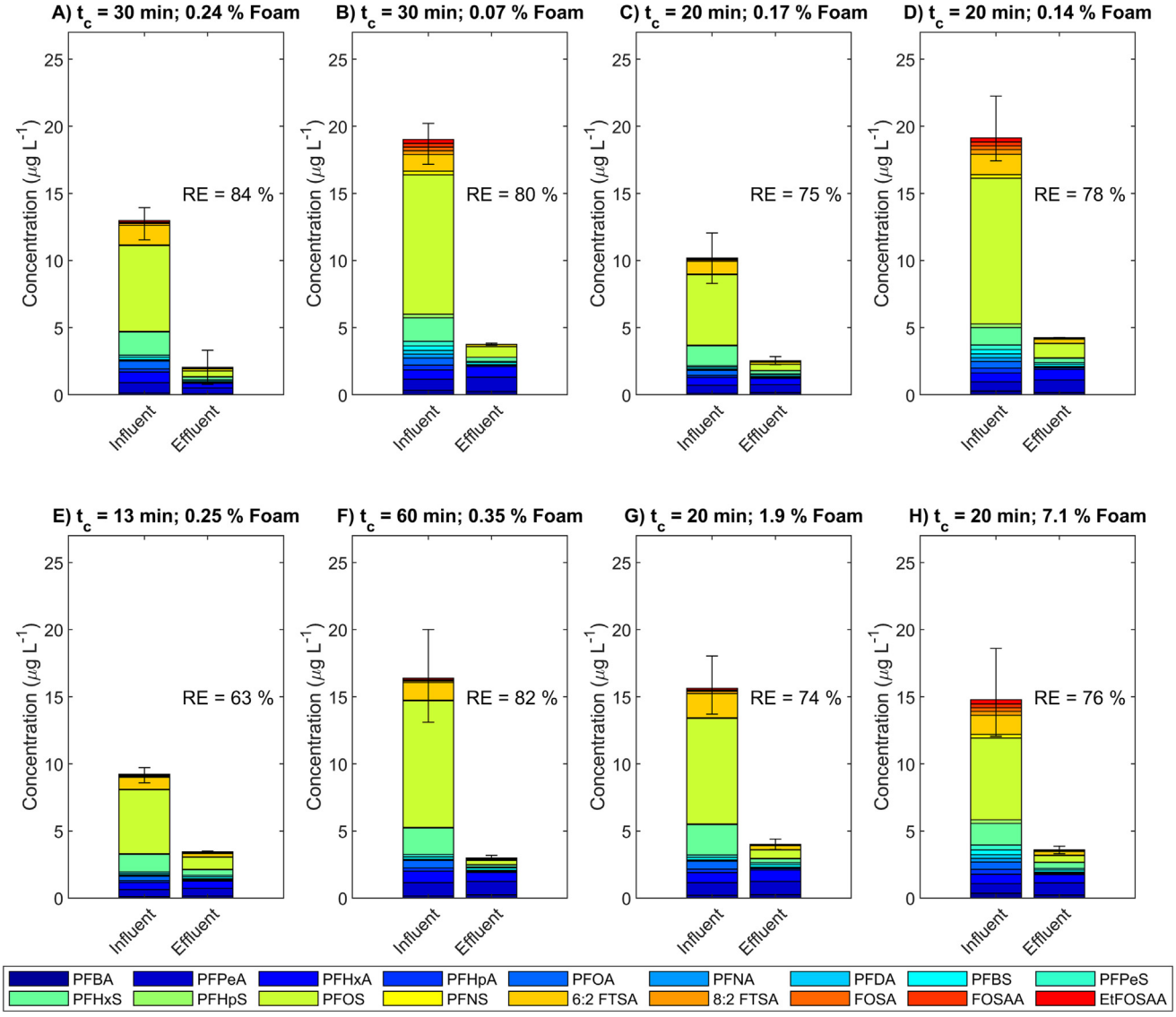

Fig. 2. Influent and effluent PFAS concentrations in different experiments, with non-detect concentrations set to 50 % of the LOQ. The repeated runs of experiments 1 (A): E1 R1 and B): E1 R2) and 2 (C): E2 R1 and D): E2 R2, see Table 1) one week in between are shown in separate subplots. Experiments 3, 4, 5 and 6 are shown in E), F), G) and H), respectively. Plot headings give the experimental t_c, which was a set variable, and the mean measured foam fraction. Plots with non-detect concentrations set to 0 and 100 % of the LOQ are given in Figs. SI 5 and 6. Error bars represent the minimum and maximum ΣPFAS concentrations found in any of the corresponding samples.

previous studies that have found optimal removal starting at contact times around 20 min (Buckley et al., 2022; Burns et al., 2021; Smith et al., 2022). Nonetheless, the mean RE increased from 76 to 82 % upon increasing the t_c from 20 to 30 min, so a positive effect of operating at higher t_c cannot be excluded. Moreover, when considering only PFOS instead of ΣPFAS in the ANOVA analysis to exclude any effects related to PFAS concentrations below the LOQ, a significant difference between the RE at 20 and 60 min t_c was found, strengthening the hypothesis that increasing the t_c above 20 min may cause a higher PFAS removal. More replicated experiments would be needed to confirm this hypothesis.

3.3. Effect of chain length and functional group on PFAS removal

The PFAS removal increased with chain length and PFSA were removed more efficiently than PFCA, as illustrated in Fig. 3. This phenomenon has been documented extensively previously (Buckley et al., 2022; Burns et al., 2021; McCleaf et al., 2021; Smith et al., 2022) and is due to a higher sorption affinity to the air-water interface of longer chain compounds and of PFSA compared to PFCA. Other long-chain PFAS such as 6:2 FTSA, 8:2 FTSA, FOSA and EtFOSAA were also removed at high efficiencies. PFNA, PFDA, PFHpS, PFNS and FOSAA were only present above the LOQ in foam samples, but not in any influent or effluent samples. Their reported removal was thus entirely based on sporadic lower LOQ values in the effluent than in the influent and is probably no accurate representation of their true removal. PFOS, PFOA, 6:2 FTSA and PFHxS had the highest mean removal efficiencies of 91 ± 5 %, 89 ± 4 %, 84 ± 7 % and 81 ± 8 %, respectively. The removal efficiency was below 30 % for PFCA with a perfluoroalkyl chain length below six and PFSA with a chain length below five. Because of this, the mean fraction of short-chain PFAS increased from 16 to 42 % from influent to effluent (min – max: 14–19 % to 26–54 %).

3.4. Effects of variations in influent water chemistry on PFAS removal

Over all eight experiments, the ΣPFAS as well as the PFOS removal efficiency correlated significantly with the influent conductivity and total elements concentration, as illustrated in Fig. 4 ($r = 0.80$, $p = 0.02$ for all). Similarly, both ΣPFAS and PFOS RE correlated significantly with the individual concentrations of Ba, K, Na and Sr ($r > 0.71$, $p < 0.05$). Expectedly, the total elements concentration and conductivity also correlated strongly with each other ($r = 0.99$, $p \approx 10^{-7}$). These results confirm

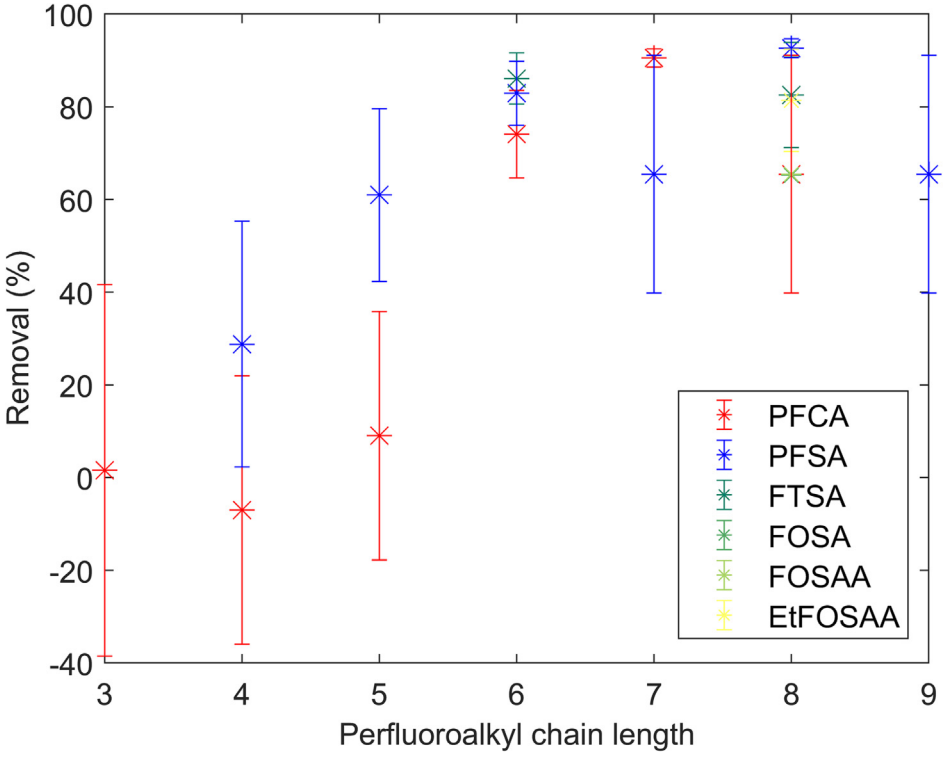

Fig. 3. Removal efficiency versus perfluoroalkyl chain length, with concentrations below the LOQ set to 50 % of the LOQ. Plots with non-detect concentrations set to 1 and 100 % of the LOQ are given in Fig. SI 7A and B. Error bars represent the standard deviation between experiments. E3 (Table 1) was excluded because of the noticeable effect of the short t_C of 13 min on the removal efficiency.

literature findings that the removal efficiency of PFAS in foam fractionation can be improved by dosing metal cation activators or increasing the ionic strength (Buckley et al., 2022; Meng et al., 2018). Moreover, they show that these effects also occur due to unintentional variations in influent water chemistry, instead of intentional dosing of metal salts. The experiment at 13 min residence time had the lowest removal efficiency as well as the lowest conductivity and total elements concentration (Fig. 4). This low removal efficiency may have been caused by a combination of these two factors, but it is not possible with our data to separate and apportion their respective effects. No significant correlations between RE and turbidity, TOC concentration or pH were found.

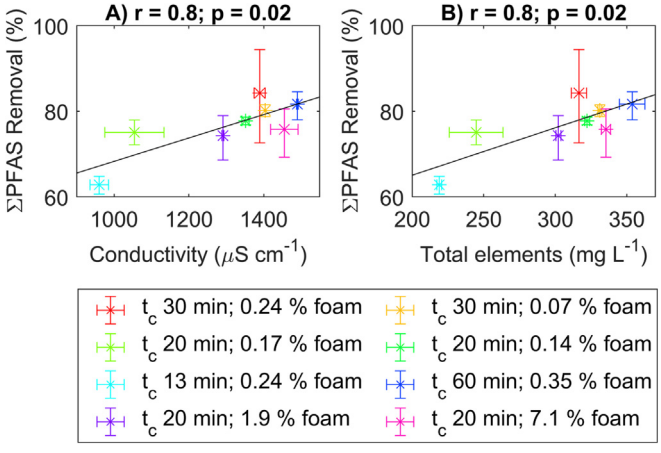

Fig. 4. ΣPFAS removal efficiency vs. conductivity and total dissolved element concentration. Horizontal error bars represent the standard deviation of A) conductivity and B) total elements concentration between experiments; vertical error bars represent the standard deviation of ΣPFAS removal between experiments.

No major differences in RE were found between the two experiments that were repeated one week apart (E1 and E2), despite higher PFAS concentrations and higher turbidity in the influent of the second runs, see Fig. 2A to D and Table SI 6. Notwithstanding the fact that dissolved elements and TOC concentrations stayed relatively similar, these minor changes in RE confirm the robustness of the treatment performance against natural variations in water quality. Conversely, the total mass balance closure decreased from 140 % in the first run to 58 % in the second run for E1, and from 98 % to 90 % for E2. These decreases in mass balance may be explained by the increased turbidity (i.e. increased adsorption to particulate matter) and the decreased foam fraction in the second runs, as outlined in Section 3.5 below.

3.5. Mass balance

The mean ΣPFAS mass balance over all experiments was 120 ± 40 % and did not differ significantly from 100 % (one-sample *t*-test), irrespective of how non-detect concentrations were handled. For non-detect concentrations set to half the LOQ, none of the mass balances for individual PFAS differed significantly from 100 % either (one-sample *t*-tests), as shown in Fig. 5. However, this conclusion changed when non-detects were handled differently, as illustrated in Fig. SI 8. Despite most mean mass balances not differing significantly from 100 %, those for certain individual compounds were below 100 % (e.g. PFBS: 86 %, PFPeS: 89 % and PFHpA: 91 %). Moreover, two experiments (E1 R2 and E2 R2, Table 1) had ΣPFAS mass balances below 100 %.

Another explanation for these low mass balance closures may be the loss of PFAS via adsorption to particulate matter. A significant negative correlation between turbidity and ΣPFAS mass balance closure was found ($r = -0.76$, $p = 0.03$. Insignificant for PFOS: $r = -0.70$, $p = 0.054$). This indicates that PFAS may have adsorbed to suspended solids in the water samples, which may have settled somewhere in the system and were thus lost from the mass balance. Turbidity further correlated with iron and aluminum content ($r = 0.97$ and 0.94, respectively, both $p < 0.0005$), which

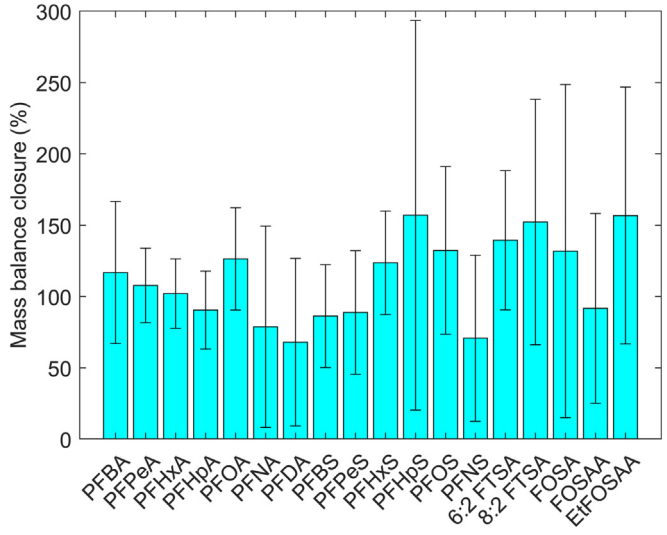

Fig. 5. Mass balance closure (%) for individual PFAS. Error bars represent the standard deviation over all experiments (n = 8).

form minerals that have a high PFAS adsorption capacity (Campos-Pereira et al., 2020; Wang and Shih, 2011; Zhang et al., 2021), further strengthening the hypothesis that PFAS may have adsorbed to suspended matter that was lost from the mass balance.

The solution used for rinsing the foam pipe after all experiments contained high PFOS, 6:2 FTSA, PFHxS and PFOA concentrations of 5700, 600, 540 and 240 μg L^{-1}, respectively. Notably, the sample also contained PFUnDA, PFDoDA, PFDS and EtFOSE (1.5, 1.1, 4.0 and 3.3 μg L^{-1}, respectively), which were not quantifiably detected in any of the other water or foam samples. Since all these four compounds are long-chained, they have high sorption coefficients (Campos-Pereira et al., 2022) and thus stick to the reactor walls rather than being transported with the foam. The full composition of this sample is given in Table SI 7. Because only one sample was collected after all tests, which probably did not contain all PFAS that were adsorbed to the pipe walls, no quantitative conclusions can be drawn on the percentage of PFAS that adsorbed to the foam pipe. Nonetheless, the high concentrations in this sample indicate that sorption to reactor parts may be an important PFAS sink.

PFOS mass balance closure correlated positively with foam fraction ($r = 0.83$, $p = 0.01$). Based on the high PFOS concentrations in the rinsing solution sample, PFOS that adsorbed to the foam pipe in experiments at low foam fractions may have been flushed out of the foam pipe at higher foam fractions. However, this correlation was not found for ΣPFAS. These results indicate that at high foam fractions, mass balance closures exceeding 100 % for especially long-chain PFAS with high sorption affinities may be caused by this rinsing effect.

For most compounds and experiments, mean mass balance closures were above 100 %, i.e. on average more PFAS was present in the foam and effluent than in the influent water. This excess of PFAS could possibly be explained by oxidative transformation of PFAS precursors that were not included in the analysis method (Houtz et al., 2016, 2013). PFCA, PFSA, FOSA and FTSA can be formed from precursors that are typically present in AFFF (Choi et al., 2022; Houtz et al., 2013), whereas EtFOSAA is generally considered a precursor compound itself (Choi et al., 2022; Houtz and Sedlak, 2012). The mean mass balance closure of EtFOSAA also exceeded 100 % (Fig. 5), which accordingly cannot be explained by precursor transformation. Probably, mass balance closures exceeding 100 % are thus also due to measurement uncertainties.

The measurement uncertainty in the PFAS concentrations reported by ALS was high, up to 40 %. When this measurement uncertainty results in reported underestimated influent concentrations or overestimated foam concentrations, the mass balance closure exceeds 100 %. A multivariable plot visualizing the sensitivity of the mass balance to these uncertainties in reported concentrations is given in Fig. SI 9. Moreover, the fluctuations in influent PFAS concentrations contributed to uncertainties in the mass balance. Nonetheless, despite these considerable measurement uncertainties, no significant differences in overall mass balance closure from 100 % were found based on all replicate analyses done in this study.

3.6. PFAS emissions to air and aerosols

The extraordinarily high recovered PFAS masses in both aerosol filters and SIP discs (see Fig. 6) clearly indicate that aerial PFAS concentrations around the reactor were much higher than normal levels in indoor air (Shoeib et al., 2008; Winkens et al., 2017). Extremely high mean ΣPFAS concentrations of 98 ng m^{-3} were measured in the air surrounding the foam fractionation reactor (sample locations 1–4, Fig. SI 1). The highest concentration of 140 ng m^{-3} was measured in the SIP disc located closest to the air outlet of the reactor (sample 4, Fig. SI 1). For comparison, the air at the reference site in the staircase of the same building had a ΣPFAS concentration of 3.6 ng m^{-3}. It should be noted that these concentrations are rough estimations based on a previously determined sampling rate (Ahrens et al., 2013), since no calibration was done in the present study.

Breakthrough through the bottom aerosol filters was low, i.e. the ΣPFAS mass measured in the top filter ranged between 0.1 % and 5 % of that in the bottom filter. The PFAS mass measured in the bottom filter clearly depended on the distance between the air outlet and the filters. 46 μg of ΣPFAS was found in the filter from the experiment in which the distance between the aerosol filter and the air outlet was decreased (E1 R2, Table 1). In comparison, over all other experiments the highest ΣPFAS mass found was only 7 μg. Based on the influent concentration of the water during each corresponding run, the highest loss of PFAS in aerosols corresponded to only 0.3 % of the entire aqueous ΣPFAS mass treated during the operation of the foam fractionation system. However, since not all air that exited the reactor passed through the filters, the actual amounts of PFAS leaving the reactor with the air were probably higher than what was caught in the aerosol filters.

The mean PFAS composition of the foam, aerosols and air was very similar, as illustrated in Fig. SI 8. For all three matrices, the main component was PFOS, at a mass-based fraction between 66 % (foam) and 77 % (aerosols), followed by PFHxS (5–13 %) and 6:2 FTSA (4–12 %). Conversely, the fraction of short-chain PFAS was only 0.7–2.6 %. In comparison, the composition of the reference air sample was slightly different, with only 43 % PFOS and 15 % short-chain PFAS. This indicates that either the

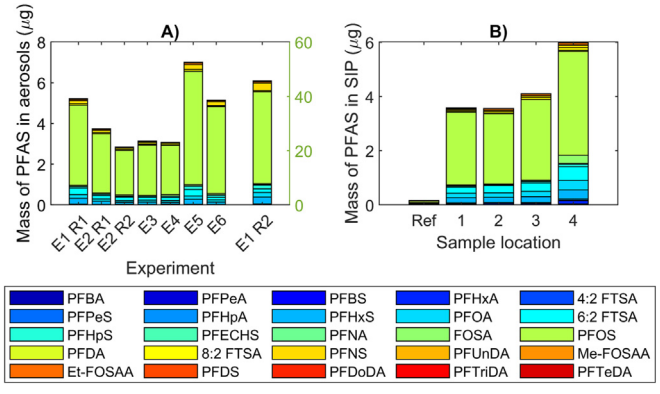

Fig. 6. Measured PFAS quantities in A) the bottom aerosol filters and B) the SIP discs. The result for the aerosol filter from experiment 1, run 2 (E1 R2) is shown on a different scale, represented by the y-axis in green on the right-side of A), to ensure readability of the data. This was the experiment during which the distance between the aerosol filter and the air outlet was decreased, causing much higher PFAS concentrations in the aerosol filter. Note that aerosol concentrations were not time-normalized, and that the duration of E4 was twice as long as the other experiments.

PFAS in the air at the reference site did not originate from the foam fractionation reactor, or that short-chain PFAS are more susceptible to transport through air than long-chain PFAS (Wong et al., 2018).

A hypothesis of this study was that high PFAS emissions in air and aerosols could explain loss of PFAS from the mass balance. Surprisingly, however, a strong positive correlation between mass balance closure and PFAS levels in the aerosol filters was found. Because of the aforementioned effect of the decreased distance between the air outlet and the filters, the results from E1 R2 were excluded from this analysis. The correlation was significant for both ΣPFAS ($r = 0.93$, $p = 0.002$) and PFOS ($r = 0.79$, $p = 0.03$). As it is improbable that a causal relationship exists between higher mass balance closure over the water phase and higher PFAS emissions in aerosols, the correlation may be explained by a common cause of the two phenomena. Possibly, both were caused by higher initial PFAS precursor concentrations and thus increased formation of target PFAS in the water as well as the aerosols. Precursor concentrations were not measured in the current study, so this could not be confirmed.

An alternative explanation relates to the role of suspended solids. PFAS-enriched aerosols are formed by bubble bursting at the air-water interface (De Leeuw et al., 2011; Sha et al., 2022), which in the foam fractionation reactor occurs mostly at the surface of the foam layer. At high suspended solids concentration, the presence of particles may impact the stability of the foam and thereby alter the collapse process, as has been discussed widely in literature (Fameau and Salonen, 2014; Kaptay and Babcsán, 2012; Petrovski et al., 2011). This altered collapse process may have resulted in lower aerosol emissions. This hypothesis is strengthened by the positive correlation between turbidity and foam concentrations ($r = 0.90$, $p = 0.003$ for ΣPFAS; $r = 0.90$, $p = 0.002$ for PFOS). An overview of these correlations is given in Fig. 7. Hence, the aforementioned positive correlation between mass balance closure and aerosol concentration was possibly caused by two separate effects at higher suspended solids concentrations: a decreased formation of PFAS-enriched aerosols and a lower mass balance closure because of PFAS loss due to sorption. However, the negative correlations of aerosol concentrations with foam concentrations and turbidity were not significant, so more research would be required to test this hypothesis.

3.6.1. Implications for worker safety

The high estimated PFAS concentrations in the air around the reactor have important implications for worker protection. The European Food Safety Authority (EFSA) includes PFOA, PFOS, PFNA and PFHxS in their recommended group tolerable weekly intake of 4.4 ng kg bodyweight^{-1} week^{-1} (EFSA, 2020). The EFSA further recommends assuming a body weight of 60 kg and an inhalation rate of 1.25 m^3 hr^{-1} for the assessment of operator exposure to plant protection products (Charistou et al., 2022). Using these same assumptions and the mean measured PFAS concentrations, an operator working a 40-h week in the room with the pilot-scale foam fractionation reactor is exposed to roughly 66 ng kg bodyweight^{-1} week^{-1} of the four PFAS included in the EFSA guidelines. This already exceeds the EFSA recommendation by a factor 15, and does not yet include PFAS exposure through diet or drinking water. On the other hand, the American Conference for Governmental Industrial Hygienists (ACGIH) has defined an occupational exposure limit for the ammonium salt of PFOA in air of 0.01 mg m^{-3} (ACGIH, 2020). The highest concentration of PFOA measured in this study was 8 ng m^{-3}, which is orders of magnitude below this limit. Nonetheless, guideline concentrations for PFAS are decreasing rapidly (Cousins et al., 2022; Post, 2021), so minimizing exposure where possible is advisable. Hence, to ensure worker safety, appropriate filters must be installed on the air outlet of pilot-scale foam fractionation reactors.

In most full-scale foam fractionation systems, the air is vented to the outside, usually already through activated carbon filters. Additionally, since the control of full-scale systems is more automated, workers are not expected to spend 40 h per week near the reactor. Accordingly,

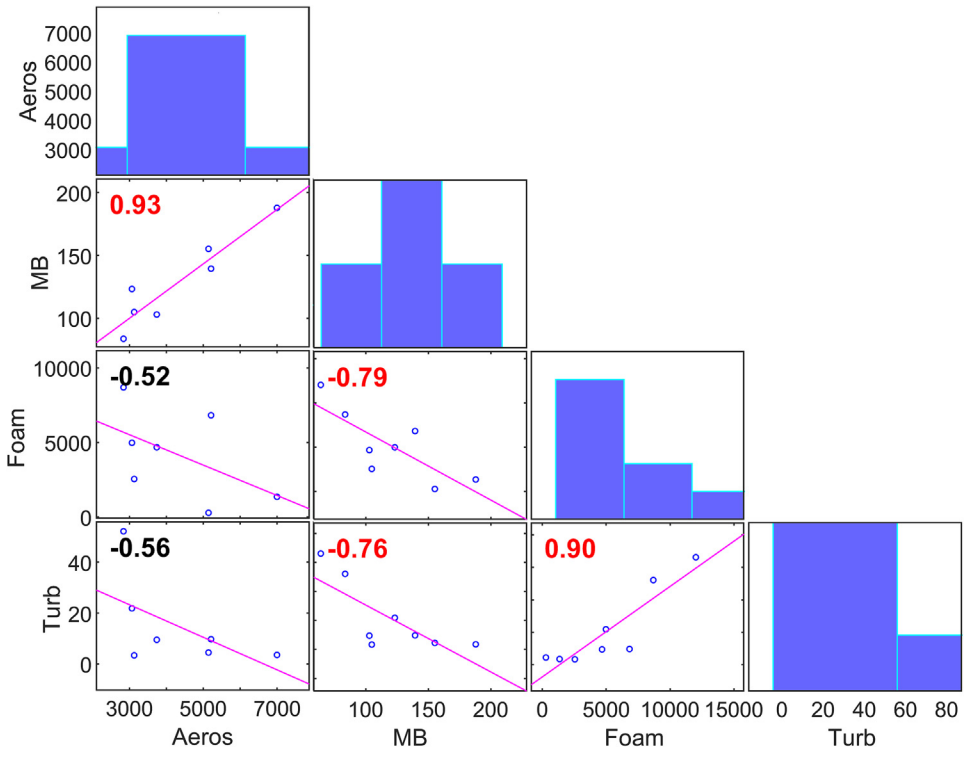

Fig. 7. Correlation matrix between aerosol concentration (Aeros, ng filter^{-1}), mass balance (MB, %), foam concentration (Foam, μg L^{-1}) and turbidity (Turb, FNU). Each data point represents the mean of one experiment. E1 R2 was excluded from the correlations with aerosol concentration, due to the strong effect of sampling aerosols closer to the air outlet. Numbers represent Pearson's correlation coefficient and are significant ($p < 0.05$) when shown in red.

the health risks demonstrated in this study are likely to be less severe for full-scale plants. Nonetheless, further research should look into the PFAS concentrations in the air around full-scale foam fractionation systems, to confirm that the safety measures are appropriate.

4. Conclusion

This study verified the high PFAS removal efficiency of a pilot scale foam fractionation system treating AFFF-contaminated industrial water. Effects of the highly variable water composition on the treatment efficiency were minimal, confirming the robustness of the technology. Nonetheless, removal efficiencies were shown to increase at higher conductivity and metal concentrations. Removal of long-chain PFAS was much higher than that of short-chain PFAS, which implies that the applicability of the technology depends on which compounds are included in guidelines and regulations. The four PFAS included in the EFSA tolerable weekly intake guideline (PFOA, PFOS, PFNA and PFHxS; EFSA, 2020) had a high combined mean removal efficiency of 90 %. Nonetheless, their mean total effluent concentration was still 1 μg L^{-1}, indicating that either a second foam fractionation step or other polishing treatments may be necessary to adequately limit human exposure to these compounds. For example, ion exchange may be used if further removal of mobile short-chain PFAS is required (Dixit et al., 2021).

There were no statistically significant differences from 100 % for individual or ΣPFAS mass balances. Nonetheless, PFAS adsorption to the walls of the reactor was found after all experiments. PFAS emissions from the air outlet of the reactor were also considerable, although they correlated positively rather than negatively with mass balance closure. These high PFAS emissions to air have important implications for the safety of operating personnel, since someone who works full-time in the room with the pilot-scale foam fractionation equipment would already have a PFAS exposure that is approximately 15 times higher than the EFSA recommendation. Moreover, PFAS that are emitted to the air rather than captured in the foam may still end up in the environment by means of long-range transport. Therefore, this study demonstrated the importance of installing adequate filters on the air outlet of foam fractionation systems.

CRediT authorship contribution statement

Sanne J. Smith: Conceptualization, Methodology, Investigation, Formal analysis, Visualization, Writing – original draft. **Jeffrey Lewis:** Conceptualization, Methodology, Resources, Writing – review & editing. **Karin Wiberg:** Writing – review & editing, Supervision, Project administration, Funding acquisition. **Erik Wall:** Writing – review & editing, Project administration. **Lutz Ahrens:** Conceptualization, Resources, Writing – review & editing, Supervision, Project administration, Funding acquisition.

Data availability

Data will be made available on request.

Declaration of competing interest

The authors declare that they have no known competing financial interests or personal relationships that could have appeared to influence the work reported in this paper.

Acknowledgements

This project has received funding from the European Union's Horizon 2020 research and innovation program under the Marie Skłodowska-Curie grant agreement No 860665 (PERFORCE3 innovative training network). We would further like to thank Svante Skarpås from Cytiva and Daniel Eriksson from ECT2 for their help with setting up the pilot system. Lastly, we thank Michael McLachlan (Stockholm University) and Angela Perez (ECT2) for their valuable comments.

Appendix A. Supplementary data

Supplementary data to this article can be found online at https://doi.org/10.1016/j.scitotenv.2023.162050.

References

ACGIH, 2020. American Conference for Governmental Industrial Hygienists TLV-TWA for Ammonium Perfluorooctanoate.
Ahrens, L., 2011. Polyfluoroalkyl compounds in the aquatic environment: a review of their occurrence and fate. J. Environ. Monit. 13, 20–31. https://doi.org/10.1039/c0em00373e.
Ahrens, L., Harner, T., Shoeib, M., Koblizkova, M., Reiner, E.J., 2013. Characterization of two passive air samplers for per- and polyfluoroalkyl substances. Environ. Sci. Technol. 47, 14024–14033. https://doi.org/10.1021/es4048945.
Belkouteb, N., Franke, V., McCleaf, P., Köhler, S., Ahrens, L., 2020. Removal of per- and polyfluoroalkyl substances (PFASs) in a full-scale drinking water treatment plant: long-term performance of granular activated carbon (GAC) and influence of flow-rate. Water Res. 182, 115913. https://doi.org/10.1016/j.watres.2020.115913.
Buck, R.C., Franklin, J., Berger, U., Conder, J.M., Cousins, I.T., Voogt, P.De, Jensen, A.A., Kannan, K., Mabury, S.A., van Leeuwen, S.P.J., 2011. Perfluoroalkyl and polyfluoroalkyl substances in the environment: terminology, classification, and origins. Integr. Environ. Assess. Manag. 7, 513–541. https://doi.org/10.1002/ieam.258.
Buckley, T., Xu, X., Rudolph, V., Firouzi, M., Shukla, P., 2021. Review of foam fractionation as a water treatment technology. Sep. Sci. Technol., 1–30 https://doi.org/10.1080/01496395.2021.1946698.
Buckley, T., Karanam, K., Xu, X., Shukla, P., Firouzi, M., Rudolph, V., 2022. Effect of mono- and di-valent cations on PFAS removal from water using foam fractionation – a modelling and experimental study. Sep. Purif. Technol. 286, 120508. https://doi.org/10.1016/j.seppur.2022.120508.
Burns, D.J., Stevenson, P., Murphy, P.J.C., 2021. PFAS removal from groundwaters using surface-active foam fractionation. Remediation 31, 19–33. https://doi.org/10.1002/rem.21694.
Campos-Pereira, H., Kleja, D.B., Sjöstedt, C., Ahrens, L., Klysubun, W., Gustafsson, J.P., 2020. The adsorption of per- and polyfluoroalkyl substances (PFASs) onto ferrihydrite is governed by surface charge. Environ. Sci. Technol. 54, 15722–15730. https://doi.org/10.1021/acs.est.0c01646.
Campos-Pereira, H., Makselon, J., Kleja, D.B., Prater, I., Kögel-Knabner, I., Ahrens, L., Gustafsson, J.P., 2022. Binding of per- and polyfluoroalkyl substances (PFASs) by organic soil materials with different structural composition – charge- and concentration-dependent sorption behavior. Chemosphere 297, 134167. https://doi.org/10.1016/j.chemosphere.2022.134167.
Casas, G., Martínez-Varela, A., Roscales, J.L., Vila-Costa, M., Dachs, J., Jiménez, B., 2020. Enrichment of perfluoroalkyl substances in the sea-surface microlayer and sea-spray aerosols in the Southern Ocean. Environ. Pollut. 267, 115512. https://doi.org/10.1016/j.envpol.2020.115512.
Charistou, A., Coja, T., Craig, P., Hamey, P., Martin, S., Sanvido, O., Chiusolo, A., Colas, M., Istace, F., 2022. Guidance on the assessment of exposure of operators, workers, residents and bystanders in risk assessment of plant protection products. EFSA J. 20, 1–134. https://doi.org/10.2903/j.efsa.2022.7032.
Choi, Y.J., Helbling, D.E., Liu, J., Olivares, C.I., Higgins, C.P., 2022. Microbial biotransformation of aqueous film-forming foam derived polyfluoroalkyl substances. Sci. Total Environ. 824. https://doi.org/10.1016/j.scitotenv.2022.153711.
Cousins, I.T., Johansson, J.H., Salter, M.E., Sha, B., Scheringer, M., 2022. Outside the safe operating space of a new planetary boundary for per- and polyfluoroalkyl substances (PFAS). Environ. Sci. Technol. 56, 11172–11179. https://doi.org/10.1021/acs.est.2c02765.
De Leeuw, G., Andreas, E.L., Anguelova, M.D., Fairall, C.W., Lewis, E.R., O'Dowd, C., Schulz, M., Schwartz, S.E., 2011. Production flux of sea spray aerosol. Rev. Geophys. 49, 1–39. https://doi.org/10.1029/2010RG000349.
Dixit, F., Dutta, R., Barbeau, B., Berube, P., Mohseni, M., 2021. PFAS removal by ion exchange resins: a review. Chemosphere 272, 129777. https://doi.org/10.1016/j.chemosphere.2021.129777.
EFSA, 2020. PFAS in food: EFSA assesses risks and sets tolerable intake [WWW Document]. URL https://www.efsa.europa.eu/en/news/pfas-food-efsa-assesses-risks-and-sets-tolerable-intake (accessed 3.17.22).
Evich, M.G., Davis, M.J.B., McCord, J.P., Acrey, B., Awkerman, J.A., Knappe, D.R.U., Lindstrom, A.B., Speth, T.F., Tebes-Stevens, C., Strynar, M.J., Wang, Z., Weber, E.J., Henderson, W.M., Washington, J.W., 2022. Per- and polyfluoroalkyl substances in the environment. Science, 375 https://doi.org/10.1126/science.abg9065.
Fameau, A.L., Salonen, A., 2014. Effect of particles and aggregated structures on the foam stability and aging. C. R. Phys. 15, 748–760. https://doi.org/10.1016/j.crhy.2014.09.009.
Fenton, S.E., Ducatman, A., Boobis, A., DeWitt, J.C., Lau, C., Ng, C., Smith, J.S., Roberts, S.M., 2020. Per- and polyfluoroalkyl substance toxicity and human health review: current state of knowledge and strategies for informing future research. Environ. Toxicol. Chem. 40, 606–630. https://doi.org/10.1002/etc.4890.
Houtz, E.F., Sedlak, D.L., 2012. Oxidative conversion as a means of detecting precursors to perfluoroalkyl acids in urban runoff. Environ. Sci. Technol. 46, 9342–9349. https://doi.org/10.1021/es302274g.
Houtz, E.F., Higgins, C.P., Field, J.A., Sedlak, D.L., 2013. Persistence of perfluoroalkyl acid precursors in AFFF-impacted groundwater and soil. Environ. Sci. Technol. 47, 8187–8195. https://doi.org/10.1021/es4018877.
Houtz, E.F., Sutton, R., Park, J.S., Sedlak, M., 2016. Poly- and perfluoroalkyl substances in wastewater: significance of unknown precursors, manufacturing shifts, and likely AFFF impacts. Water Res. 95, 142–149. https://doi.org/10.1016/j.watres.2016.02.055.

Kaptay, G., Babcsán, N., 2012. Particle stabilized foams. In: Stevenson, P. (Ed.), Foam Engineering: Fundamentals and Applications. John Wiley & Sons Ltd, Chichester, UK, pp. 121–143 https://doi.org/10.1002/9781119954620.ch7.

Lee, Y.C., Wang, P.Y., Lo, S.L., Huang, C.P., 2017. Recovery of perfluorooctane sulfonate (PFOS) and perfluorooctanoate (PFOA) from dilute water solution by foam flotation. Sep. Purif. Technol. 173, 280–285. https://doi.org/10.1016/j.seppur.2016.09.012.

Lenka, S.P., Kah, M., Padhye, L.P., 2021. A review of the occurrence, transformation, and removal of poly- and perfluoroalkyl substances (PFAS) in wastewater treatment plants. Water Res. 199, 117187. https://doi.org/10.1016/j.watres.2021.117187.

McCleaf, P., Kjellgren, Y., Ahrens, L., 2021. Foam fractionation removal of multiple per- and polyfluoroalkyl substances from landfill leachate. AWWA Water Sci. 3, 1–14. https://doi.org/10.1002/aws2.1238.

Meng, P., Deng, S., Maimaiti, A., Wang, B., Huang, J., Wang, Y., Cousins, I.T., Yu, G., 2018. Efficient removal of perfluorooctane sulfonate from aqueous film-forming foam solution by aeration-foam collection. Chemosphere 203, 263–270. https://doi.org/10.1016/j.chemosphere.2018.03.183.

Petrovski, S., Dyson, Z.A., Quill, E.S., McIlroy, S.J., Tillett, D., Seviour, R.J., 2011. An examination of the mechanisms for stable foam formation in activated sludge systems. Water Res. 45, 2146–2154. https://doi.org/10.1016/j.watres.2010.12.026.

Post, G.B., 2021. Recent US state and federal drinking water guidelines for per- and polyfluoroalkyl substances. Environ. Toxicol. Chem. 40, 550–563. https://doi.org/10.1002/etc.4863.

Sha, B., Johansson, J.H., Tunved, P., Bohlin-Nizzetto, P., Cousins, I.T., Salter, M.E., 2022. Sea spray aerosol (SSA) as a source of perfluoroalkyl acids (PFAAs) to the atmosphere: field evidence from long-term air monitoring. Environ. Sci. Technol. 56, 228–238. https://doi.org/10.1021/acs.est.1c04277.

Shoeib, M., Harner, T., Sum, C.L., Lane, D., Zhu, J., 2008. Sorbent-impregnated polyurethane foam disk for passive air sampling of volatile fluorinated chemicals. Anal. Chem. 80, 675–682. https://doi.org/10.1021/ac701830s.

Smith, S.J., Wiberg, K., McCleaf, P., Ahrens, L., 2022. Pilot-scale continuous foam fractionation for the removal of per- and polyfluoroalkyl substances (PFAS) from landfill leachate. ACS ES&T Water 2, 841–851. https://doi.org/10.1021/acsestwater.2c00032.

Sunderland, E.M., Hu, X.C., Dassuncao, C., Tokranov, A.K., Wagner, C.C., Allen, J.G., 2019. A review of the pathways of human exposure to poly- and perfluoroalkyl substances (PFASs) and present understanding of health effects. J. Expo. Sci. Environ. Epidemiol. 29, 131–147. https://doi.org/10.1038/s41370-018-0094-1.

US EPA, 2016. Drinking Water Health Advisories for PFOA and PFOS [WWW Document]. URL (accessed 4.14.22) https://www.epa.gov/ground-water-and-drinking-water/drinking-water-health-advisories-pfoa-and-pfos.

Wang, F., Shih, K., 2011. Adsorption of perfluorooctanesulfonate (PFOS) and perfluorooctanoate (PFOA) on alumina: influence of solution pH and cations. Water Res. 45, 2925–2930. https://doi.org/10.1016/j.watres.2011.03.007.

Winkens, K., Koponen, J., Schuster, J., Shoeib, M., Vestergren, R., Berger, U., Karvonen, A.M., Pekkanen, J., Kiviranta, H., Cousins, I.T., 2017. Perfluoroalkyl acids and their precursors in indoor air sampled in children's bedrooms. Environ. Pollut. 222, 423–432. https://doi.org/10.1016/j.envpol.2016.12.010.

Wong, F., Shoeib, M., Katsoyiannis, A., Eckhardt, S., Stohl, A., Bohlin-Nizzetto, P., Li, H., Fellin, P., Su, Y., Hung, H., 2018. Assessing temporal trends and source regions of per- and polyfluoroalkyl substances (PFASs) in air under the Arctic Monitoring and Assessment Programme (AMAP). Atmos. Environ. 172, 65–73. https://doi.org/10.1016/j.atmosenv.2017.10.028.

Zhang, Z., Sarkar, D., Datta, R., Deng, Y., 2021. Adsorption of perfluorooctanoic acid (PFOA) and perfluorooctanesulfonic acid (PFOS) by aluminum-based drinking water treatment residuals. J. Hazard. Mater. Lett. 2, 100034. https://doi.org/10.1016/j.hazl.2021.100034.